

Efficient Adversarial Input Generation via Neural Net Patching

Tooba Khan, Kumar Madhukar, Subodh Vishnu Sharma

Indian Institute of Technology Delhi, India

Abstract

The adversarial input generation problem has become central in establishing the robustness and trustworthiness of deep neural nets, especially when they are used in safety-critical application domains such as autonomous vehicles and precision medicine. This is also practically challenging for multiple reasons – scalability is a common issue owing to large-sized networks, and the generated adversarial inputs often lack important qualities such as naturalness and output-impartiality. We relate this problem to the task of patching neural nets, i.e. applying *small* changes in some of the network’s weights so that the modified net satisfies a given property. Intuitively, a patch can be used to produce an adversarial input because the effect of changing the weights can also be brought about by changing the inputs instead. This work presents a novel technique to patch neural networks, and an innovative approach of using it to produce perturbations of inputs which are adversarial for the original net. We note that the proposed solution is significantly more effective than the prior state-of-the-art techniques.

Introduction

Deep Neural Networks (DNNs) today are omnipresent. An important reason behind their widespread use is their ability to generalize and thereby perform well even on previously unseen inputs. While this is a great practical advantage, it may sometimes make DNNs unreliable. In safety- or business-critical applications this lack of reliability can indeed have dreadful costs. Evidently, central to a trained network’s unreliability lies the lack of robustness against input perturbations, *i.e.*, small changes to some inputs cause a substantial change in the network’s output. This is undesirable in many application domains. For example, consider a network that has been trained to issue advisories to aircrafts to alter their paths based on approaching intruder aircrafts. It is natural to expect such a network to be robust in its decision-making, *i.e.* the advisory issued for two very similar situations should not be vastly different. At the same time, if that is not the case, then demonstrating the lack of robustness through *adversarial inputs* can help not only in improving the network but also in deciding when the network should relinquish control to a more dependable entity.

Given a network and an input, an adversarial input is one which is *very close* to the given input and yet the network’s outputs for the two inputs are quite different. In the

last several years, there has been much work on finding adversarial inputs (Pei et al. 2017; Guo et al. 2018; Goodfellow, Shlens, and Szegedy 2015; Kurakin, Goodfellow, and Bengio 2017; Alparslan et al. 2021). These approaches can be divided into black-box and white-box methods based on whether they consider the network’s architecture during the analysis or not. A variety of techniques have been developed in both these classes, ranging from generation of random attacks (Goodfellow, Shlens, and Szegedy 2015; Kurakin, Goodfellow, and Bengio 2017) and gradient-based methods (Alparslan et al. 2021) to symbolic execution (Wang et al. 2018; Yang et al. 2021; Li et al. 2019), fault localization (Eniser, Gerasimou, and Sen 2019), coverage-guided testing (Pei et al. 2017; Guo et al. 2018), and SMT and ILP solving (Gopinath et al. 2018). However, there are several issues that limit the practicability of these techniques – poor success rate, large distance between the adversarial and the original input (both in terms of the number of input values changed, and the degree of the change), unnatural or perceptibly different inputs, and output partiality (techniques’ bias to produce adversarial examples for just one of the network’s outputs). This paper presents a useful approach to generate adversarial inputs in a way that addresses these issues.

We relate the problem of finding adversarial inputs to the task of patching neural nets, *i.e.* applying small changes in some of the network’s weights so that the modified net satisfies a given property. Patching DNNs is a topic of general interest to the Machine Learning community because of its many applications, which include bug-fixing, watermark resilience, and fine-tuning of DNNs, among others (Goldberger et al. 2020). Intuitively, the relation between these two problems is based on the observation that a patch can be translated into an adversarial input because the effect of changing the weights may be brought about by changing the inputs instead. In fact, a patch in the very first *edge-layer* of a network can very easily be transformed into a corresponding change in the input by just solving linear equations. While there are techniques to solve the patching problem (Goldberger et al. 2020; Refaeli and Katz 2021), it is in general a difficult task, particularly for layers close to the input layer. Informally, this is because the computation of the entire network needs to be encoded and passed to a constraint solver in order to obtain a patch. For large-sized networks, this gives rise to a big monolithic constraint lead-

ing to scalability issues for the solver. We address this by proposing an improvement in the technique of (Goldberger et al. 2020), and then using it repeatedly to find a middle-layer patch and chop off the latter half of the network, till a first-layer patch has been obtained. Our experiments on three popular image-dataset benchmarks show that our approach does significantly better than other state-of-the-art techniques, in terms of the number of pixels modified as well as the magnitude of the change. This reflects in the quality of the adversarial images, both visually and in several qualitative metrics that we present later.

The core contributions of this paper are:

- A novel technique to patch neural networks, and an innovative approach of using it to produce small perturbations of inputs which are adversarial for the original net.
- An extensive experimental evaluation using CIFAR-10 (Krizhevsky and Hinton 2009), MNIST (Deng et al. 2009a), and ImageNet (Deng et al. 2009b) datasets, and a number of qualitative parameters, to show the efficacy of our approach over the state-of-the-art.

Illustrative Example

Let us consider a toy DNN, \mathcal{N} , shown in Fig. 1. It has two neurons in each of its four layers – the input layer first, followed by two hidden layers, and then the output layer. We assume that the hidden layers have ReLU¹ as the activation function. For neurons without an activation function, the value of a neuron is computed by summing up, for each incoming edge to the neuron, the product of the edge weight and the value of the neuron at the edge’s source. In presence of an activation function, the value is computed by applying the function on this sum. For example, for the input $\langle 0.5, 0.5 \rangle$, the values at the next three layers are $\langle 1, 0.5 \rangle$, $\langle 3.5, 1.5 \rangle$, and $\langle -5, -6.5 \rangle$ respectively.

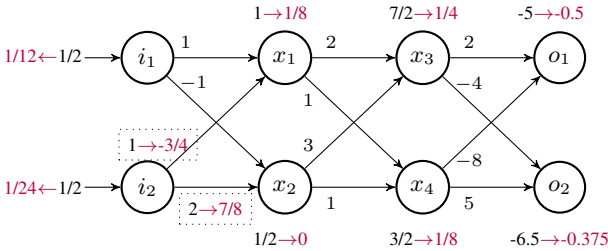


Figure 1: Adversarial inputs from first-layer modification. The adversarial input and the corresponding values of each neuron are written in red. The modification required in first layer weights are shown in black boxes.

Finding an adversarial input $\langle i_1, i_2 \rangle$ for the input $\langle 0.5, 0.5 \rangle$ amounts to finding a value for each i_k ($k \in \{1, 2\}$) such that $|i_k - 0.5| \leq \delta$ and the corresponding output $o_2 > o_1$, for a given small δ . It is noteworthy that if we want the second output to become bigger than the first one, this can be achieved by modifying the weights instead of the inputs. For

example, if the edges connecting the second input neuron to the first hidden layer had the weights $\langle -0.75, 0.875 \rangle$ instead of $\langle 1, 2 \rangle$, then the next three layers would have the values $\langle 0.125, 0 \rangle$, $\langle 0.25, 0.125 \rangle$, and $\langle -0.5, -0.375 \rangle$, and our goal would be met by modifying the weights while keeping the inputs unchanged. We will come to the question of how to find the changed first-layer weights in a bit, but let us first see how the changed weights can help us obtain an adversarial input. This is a rather simple exercise. Note that with the changed weights, the values of the neurons in the first hidden layer were $\langle 0.125, 0 \rangle$. So, our task is simply to find inputs for which the first hidden layer values stay as $\langle 0.125, 0 \rangle$, but with the original weights $\langle 1, 2 \rangle$. This can be done by solving the following equations, where δ_1 and δ_2 ($\delta_1, \delta_2 \leq \delta \leq 0.5$, say) are the changes in the two inputs respectively.

$$(1/2 + \delta_1) + (1/2 + \delta_2) = 1/8 \quad (1)$$

$$-(1/2 + \delta_1) + 2 * (1/2 + \delta_2) = 0 \quad (2)$$

We get $\delta_1 = -5/12, \delta_2 = -11/24$ and, thus, the adversarial input as $\langle 1/12, 1/24 \rangle$. The dotted rectangles in Fig. 1 contain the adversarial inputs and the corresponding values at each layer.

The first thing to notice here is that Eqn. 2 could have been relaxed as $-(1/2 + \delta_1) + 2 * (1/2 + \delta_2) \leq 0$ because of the ReLU activation function. This may give us smaller values of δ_i ’s. Moreover, along with minimizing the change in each input pixel, we can also minimize the number of pixels that are modified, as shown here.

$$(1/2 + \delta_1 * M_1) + (1/2 + \delta_2 * M_2) = 1/8 \quad (3)$$

$$-(1/2 + \delta_1 * M_1) + 2 * (1/2 + \delta_2 * M_2) \leq 0 \quad (4)$$

$$M_1, M_2 \in \{0, 1\}; \text{ minimize } \sum M_i \quad (5)$$

In practice, we solve these constraints in place of Eqns. 1-2; this gives us better adversarial inputs.

There are a few more points to note before we proceed. First, it is only the first-layer modification that may be easily translated into an adversarial input as illustrated. Modification in deeper layers are not immediately helpful; they cannot be translated easily into an adversarial input because of the non-linear activation functions. Second, we need to find *small* modifications in the weights, so that the corresponding δ_i ’s in the inputs fall within the allowed δ . And, lastly, while there are ways to compute a first-layer change directly using an SMT or an ILP solver (Goldberger et al. 2020), this approach is not very scalable in practice as large-sized networks give rise to big monolithic formulas that may be difficult for the solver. Instead, we propose an iterative approach that finds a middle-layer modification using (Goldberger et al. 2020)² and chops off the latter half of the network, repeatedly till a first-layer patch is found.

Since our network has three edge-layers, we start by finding a small modification of the weights in the second edge-layer with which we can achieve our target of making o_2 bigger than o_1 for the input $\langle 0.5, 0.5 \rangle$. We propose an $\epsilon_{i,j}$

¹ReLU(x) = max($0, x$)

²In fact, we use an improved version of this which is described in the next section.

change in the weight of the j^{th} edge in i^{th} edge-layer, and encode the constraints for $o_2 > o_1$ as follows:

$$x_3 = \max(0, 1 * (2 + \epsilon_{2,1}) + 1/2 * (3 + \epsilon_{2,2})) \quad (6)$$

$$x_4 = \max(0, 1 * (1 + \epsilon_{2,3}) + 1/2 * (1 + \epsilon_{2,4})) \quad (7)$$

$$-4 * x_3 + 5 * x_4 > 2 * x_3 - 8 * x_4 \quad (8)$$

The range of each $\epsilon_{i,j}$ is $[-\alpha, \alpha]$ if α is the biggest permissible modification for an edge-weight. We minimize the magnitude of the total change using Gurobi (Gurobi Optimization, LLC 2022). For the equations above, we get $\langle \epsilon_{2,1}, \epsilon_{2,2}, \epsilon_{2,3}, \epsilon_{2,4} \rangle = \langle -9/8, -17/4, -5/4, -1/4 \rangle$. These changes indeed make the second output bigger (see Fig. 2).

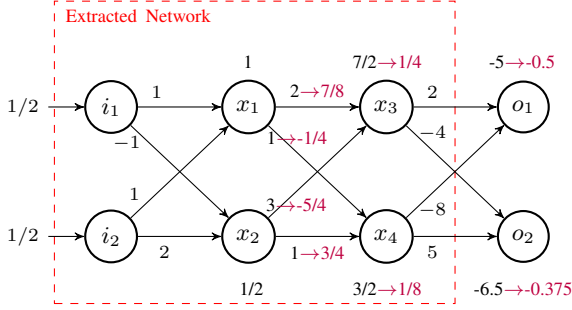


Figure 2: Middle-layer modification and sub-net extraction

Our next step is to extract a sub-network (see Fig. 2) and look for a modification in its middle layer. Since the extracted network has only two edge-layers, this step will give us a first-layer modification. The equations, subject to the constraint that x_3 and x_4 get the values $1/4$ and $1/8$ respectively, are shown below.

$$x_1 = \max(0, 1/2 * (1 + \epsilon_{1,1}) + 1/2 * (1 + \epsilon_{1,2})) \quad (9)$$

$$x_2 = \max(0, 1/2 * (-1 + \epsilon_{1,3}) + 1/2 * (2 + \epsilon_{1,4})) \quad (10)$$

$$2 * x_1 + 3 * x_2 = 1/4; \quad 1 * x_1 + 1 * x_2 = 1/8 \quad (11)$$

Gurobi gives us the solution $\langle \epsilon_{1,1}, \epsilon_{1,2}, \epsilon_{1,3}, \epsilon_{1,4} \rangle = \langle 0, -7/4, 0, -9/8 \rangle$, from which we can obtain the adversarial input $\langle 1/12, 1/24 \rangle$ as already shown above.

Methodology

We now describe the technical details of our approach and present our algorithm. We begin with the notation that we use. Let \mathcal{N} denote the DNN that we have with n inputs (i_1, i_2, \dots, i_n), m outputs (o_1, o_2, \dots, o_m), and k layers (l_1, l_2, \dots, l_k). We use $v_{p,q}$ to denote the value of the q^{th} neuron in l_p . We assume that \mathcal{N} is feed-forward, i.e., the (weighted) edges connect neurons in adjacent layers only, and point in the direction of the output layer. We use the term *edge-layer* to refer to all the edges between any two adjacent layers of \mathcal{N} , and denote the edge layers as $el_1, el_2, \dots, el_{k-1}$. We also assume the hidden layers (l_2, l_3, \dots, l_{k-1}) in \mathcal{N} have ReLU activation function, and that there is no activation function on any output neuron.

For simplicity, we assume that the neurons do not have any biases. This is not a limitation in any sense; our implementation handles them directly. Moreover, a DNN with biases can be converted into an equivalent one without any biases. Like in the previous section, we use δ_p to denote the change in the p^{th} input, and $\epsilon_{q,s}$ to denote the change in the weight of the q^{th} edge in el_s . The δ_p 's are constrained to be $\leq \delta$, which is the biggest perturbation allowed in any pixel to find an adversarial input.

Algorithm 1 presents a pseudocode of our algorithm. The inputs to the algorithm are: \mathcal{N} , δ , and the values for the input neurons $v_{1,1}, v_{1,2}, \dots, v_{1,n}$, for which the corresponding output does not satisfy a given adversarial property $\phi(o_1, o_2, \dots, o_m)$ (denoted simply as ϕ , henceforth). The aim of our algorithm is to find a new set of input values $v'_{1,1}, v'_{1,2}, \dots, v'_{1,n}$ such that \mathcal{N} 's output corresponding to these new inputs satisfies ϕ . The algorithm works in the following two steps. First, it finds a *small* modification in the weights of el_1 to derive \mathcal{N}_{mod} (which is essentially \mathcal{N} with the modified weights in el_1), such that the output of \mathcal{N}_{mod} for the input $v_{1,1}, v_{1,2}, \dots, v_{1,n}$ satisfies ϕ . Then, the algorithm translates this first-layer modification into adversarial inputs $v'_{1,1}, v'_{1,2}, \dots, v'_{1,n}$, subject to the constraint that $|v'_{1,p} - v_{1,p}| \leq \delta$, for every $p \in [1, n]$. This second step is shown in the algorithm as the function *mod2adv*, the pseudocode of which has been omitted as this is a simple call to Gurobi as illustrated in the previous section.

Let us assume for the time being that we have a sub-routine *modifyEdgeLayer* that takes as input a DNN \mathcal{N} , one of its edge-layers el_k , values of the input neurons $v_{1,1}, v_{1,2}, \dots, v_{1,n}$, and a property ϕ on the output layer neurons, and returns a new network \mathcal{N}_{mod} with the constraints that:

- \mathcal{N}_{mod} is same as \mathcal{N} except for the weights in el_k , and
- the output of \mathcal{N}_{mod} on $v_{1,1}, v_{1,2}, \dots, v_{1,n}$ satisfies ϕ .

Clearly, with such a sub-routine, the first step of our algorithm becomes trivial. We would simply call *modifyEdgeLayer* with the given input, \mathcal{N} , ϕ , and el_1 . We refer to the work of Goldberger et al. (Goldberger et al. 2020) which gives us exactly this. However, we do not use it directly to find our first-layer modification. Informally, the technique of (Goldberger et al. 2020) uses variables $\epsilon_{q,s}$ to denote the changes in the weights (in a given edge-layer s) and encodes the computation of the entire network, and then adds the constraint that the output must satisfy ϕ . It then uses Gurobi on these constraints, to solve for (and optimize) the values of $\epsilon_{q,s}$. Consider an example (reproduced from (Goldberger et al. 2020)) shown in Fig. 3 with the output property $\phi := (v_{3,1} \geq v_{3,2})$. Let us ignore the color of the output neurons for now. If the input neurons are given values $v_{1,1} = 3$ and $v_{1,2} = 4$, the output neurons get the value $v_{3,1} = -2$ and $v_{3,2} = 2$, which does not satisfy ϕ . Note that the hidden layer neurons have ReLU activation function. In order to obtain a second edge-layer modification such that ϕ holds for the input $\langle 3, 4 \rangle$, the technique of (Goldberger et al. 2020) generates the following constraints.

In a similar way, the constraints can be generated for modification in any layer, by propagating the input values up to

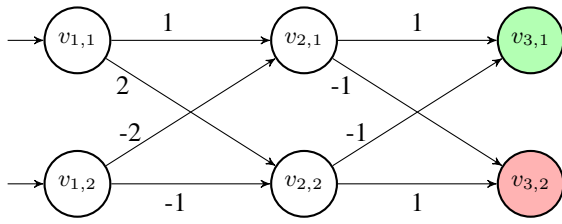


Figure 3: Example illustrating DNN modification, from (Goldberger et al. 2020)

$$\text{minimize } M \quad (12)$$

$$M \geq 0 \quad (13)$$

$$-M \leq \epsilon_{1,2} \leq M \quad (14)$$

$$-M \leq \epsilon_{2,2} \leq M \quad (15)$$

$$-M \leq \epsilon_{3,2} \leq M \quad (16)$$

$$-M \leq \epsilon_{4,2} \leq M \quad (17)$$

$$v_{3,1} = 0.(1 + \epsilon_{1,2}) + 2.(-1 + \epsilon_{2,2}) \quad (18)$$

$$v_{3,2} = 0.(-1 + \epsilon_{3,2}) + 2.(1 + \epsilon_{4,2}) \quad (19)$$

$$v_{3,1} \geq v_{3,2} \quad (20)$$

Figure 4: DNN modification constraints for Fig.3

that layer, encoding the computation from there onward, and adding the output property ϕ . If a first-layer modification has to be found, this gives rise to a big monolithic constraint, particularly for large-sized networks. This does not scale in practice, and therefore we propose an iterative approach of doing this in our algorithm. The iterative approach uses the above technique to find a middle-layer modification, derive a new output property ϕ' for the first half of the network, and does this repeatedly till a first-layer modification is found. This has been illustrated in the function *findFirstLayerMod* in Alg. 1, which calls *modifyEdgeLayer* in a loop. The last bit here is to understand how the modified output property ϕ' may be derived in each iteration. The way this works is as follows. Let us say that the last call to *modifyEdgeLayer* was made on edge-layer $el_{(j-1)}$, which connects the layers $l_{(j-1)}$ and l_j . We can use the modified weights to propagate the inputs all the way to layer l_j , by simply simulating the network on the inputs. This gives us values for all the neurons in layer l_j , say c_1, c_2, \dots and so on. Now, the modified weights are replaced by the original weights, and all the layers after l_j are dropped off from the network. This reduced network \mathcal{N}' has exactly the layers l_1 to l_j of \mathcal{N} . We denote this reduction as $\mathcal{N} \downarrow_{(l_1 \dots l_j)}$. Ideally, we would want to find a middle-layer modification in \mathcal{N}' under the new output constraint as $\phi' := (v_{j,1} = c_1) \wedge (v_{j,2} = c_2) \wedge \dots$ and so on. The updated ϕ' is correct because we know that ϕ gets satisfied when these values are propagated further to the output layer. But, we can relax the strict equalities of ϕ' into inequalities as discussed in the next subsection.

Algorithm 1: Adversarial Inputs via Network Patching

Input: $\mathcal{N}, l, \delta, \phi$, and input $\langle v_{1,1}, \dots, v_{1,n} \rangle$

Output: Adversarial input $\langle v'_{1,1}, \dots, v'_{1,n} \rangle$

findFirstLayerMod(\mathcal{N}, l, in, ϕ):

```

1: while true do
2:    $p \leftarrow \lceil (l/2) \rceil$ 
3:    $\mathcal{N}_{mod} \leftarrow \text{modifyEdgeLayer}(\mathcal{N}, in, \phi, el_p)$ 
4:   return  $\mathcal{N}_{mod}$  if ( $p = 1$ )
5:    $\langle c_1, c_2, \dots \rangle \leftarrow \text{simulate}(\mathcal{N}_{mod}, in)$ 
6:    $\phi' = (v_{(p+1),1} = c_1) \wedge (v_{(p+1),2} = c_2) \wedge \dots$ 
7:    $\mathcal{N}' = \mathcal{N} \downarrow_{(l_1 \dots l_{(p+1)})}$ 
8:    $\mathcal{N} \leftarrow \mathcal{N}'; l \leftarrow (p + 1); \phi \leftarrow \phi'$ 
9: end while
```

main():

```

1:  $in \leftarrow \langle v_{1,1}, \dots, v_{1,n} \rangle$ 
2:  $\mathcal{N}_{mod} \leftarrow \text{findFirstLayerMod}(\mathcal{N}, l, in, \phi)$ 
3:  $\langle \delta_1, \delta_2, \dots, \delta_n \rangle = \text{mod2adv}(\mathcal{N}_{mod}, in, \delta)$ 
4:  $\langle v'_{1,1}, \dots, v'_{1,n} \rangle = \langle v_{1,1}, \dots, v_{1,n} \rangle + \langle \delta_1, \dots, \delta_n \rangle$ 
5: return  $\langle v'_{1,1}, \dots, v'_{1,n} \rangle$ 
```

Simplifying DNN Modification Constraints

Let us revisit the example of Fig. 3, and the constraints corresponding to the modification problem shown in Fig. 4. Recall that the modification problem in this example was to find small changes in the weights of the second edge-layer, such that $v_{3,1} \geq v_{3,2}$ for the input $\langle 3, 4 \rangle$. This is not true for the DNN in this example as $v_{3,1}$ gets the value -2, whereas $v_{3,2}$ gets the value 2. A possible way of satisfying $v_{3,1} \geq v_{3,2}$ is to change weights in such a way that $v_{3,1}$ decreases and $v_{3,2}$ increases. This can give us a marking of the final layer neurons as decrement and increment, which has been indicated by the neuron colors red and green in Fig. 3. The useful thing about such a marking is that it can be propagated backward to other layers. For instance, in the same example, $v_{2,1}$ and $v_{2,2}$ can also be colored green and red, resp. This works by looking at the edge weights. Since $v_{2,1}$ is connected to $v_{3,1}$ with a positive-weight edge, an increase in $v_{3,1}$ can be brought about by increasing $v_{2,1}$. If we look at $v_{2,2}$, since it connected to $v_{3,1}$ with a negative-weight edge, a decrease in $v_{2,2}$ would result in an increase in $v_{3,1}$. This marking was proposed by Elboher et al. (Elboher, Gottschlich, and Katz 2020), although it was in the context of abstraction-refinement of neural networks. We refer the interested readers to (Elboher, Gottschlich, and Katz 2020) for more details about this marking scheme. In what follows, we explain how this marking can be useful in simplifying the modification constraints.

Since we are interested in modifying weights in the second edge-layer (el_2), we propagate the inputs to the second layer of neurons. This gives us the values $\langle 0, 2 \rangle$ for $\langle v_{2,1}, v_{2,2} \rangle$. Having propagated the input to the source neurons of el_2 , and the increment-decrement marking at the target neurons of el_2 , we claim that we can identify whether a given edge-weight should be increased, or decreased. Let

us consider the edge between $v_{2,2}$, which has a value of 2, and $v_{3,1}$, which has an increment marking. We claim that the change in this edge, $\epsilon_{2,2}$ should be positive. Naturally, since the value is positive, we should multiply with a *bigger* weight to get an increased output. Instead, if a positive value was connected to a decrement neuron, we should decrease the weight (for example, for the edge between $v_{2,2}$ and $v_{3,2}$). In case of negative values, just the opposite needs to be done. And if the value is zero, no change needs to be made at all. With this, the constraints in Fig. 4 get simplified as $\epsilon_{1,2} = \epsilon_{2,2} = 0, 0 \leq \epsilon_{3,2} \leq M$ and $-M \leq \epsilon_{3,2} \leq 0$. We have implemented this on top of the tool corresponding to (Goldberger et al. 2020) and used it in our call to *modifyEdgeLayer*.

We end this section with a brief note on how this increment-decrement marking may help us relax the modified output property ϕ' . Recall that ϕ' was derived as a conjunction of equality constraints, where each conjunct was equating a last-layer neuron of the reduced network with the values obtained by simulating the input on \mathcal{N}_{mod} . Since we know the increment-decrement marking of last layer neurons, we can relax each conjunct into an inequality by replacing the equality sign with \leq (\geq) for decrement (increment) neurons. This allows us to obtain, possibly better, solutions more often.

Related Work

Robustness of DNNs has gained a lot of attention in the last several years as DNNs are permeating our lives, even safety- and business-critical aspects of it. A number of techniques have been developed to establish robustness or demonstrate the lack of it through adversarial examples. These techniques may be broadly classified as black box and white box approaches.

Black box methods do not consider the architecture of DNNs in trying to argue about its robustness. Attacks based on the L2 and L0 norms were introduced in (Alparslan et al. 2021). These attacks change the pixel values by some fixed amount, and measure their effectiveness by the decrease in confidence of the original label. Fast Gradient sign method (Goodfellow, Shlens, and Szegedy 2015) is a gradient based method, which uses gradient of the loss of neural network when the original and modified images are fed to it. These methods modify a large number of pixels in the original image, to induce a misclassification. Changing more pixels makes the adversarial image visibly different from the original image.

White box methods, on the other hand, involve looking at the complete architecture of the DNNs to obtain adversarial inputs or argue that none exists. Verification of neural networks using Symbolic execution is one such white box approach. As discussed in (Gopinath et al. 2018), it translates the neural network into an imperative program, and uses SMT (Symbolic Modulo Theory) based solver to prove given properties. However, such techniques are not scalable due to exponential time complexity. Symbolic propagation is another white box method which converts inputs to symbolic representations and propagates them through the hidden layers and the output layer. (Li et al. 2019)] uses symbolic prop-

agation along with abstract interpretation to compute bounds on the neurons. (Wang et al. 2018) has used integer arithmetic to find bounds on the outputs. (Yang et al. 2021) verifies local robustness properties using symbolic propagation and global robustness properties using Lipschitz constant based framework. However, these techniques often given loose bounds and lack precision.

Another white box technique is to find flaws in the training phase of the neural network such as the use of an inappropriate loss function. The most popularly used loss function while training classification networks is softmax cross entropy loss. The authors of (Pang et al. 2020) claim that the presence of adversarial behavior in a deep neural network can be attributed to its loss function. They propose Max-Mahalanobis center (MMC) loss which learns from dense feature regions in the input images. (Raj Dhamija, Gunther, and Boulton 2019) has proposed two loss functions: Entropic Open-Set Loss and Objectosphere Loss. Entropic Open-Set Loss makes the softmax values of all classes uniform when the input is unknown. Objectosphere Loss increases the boundary of feature magnitudes of known and unknown samples. Loss function replacement techniques are still vulnerable to adversarial attacks. They can not be transferred either. These methods cannot be used to test the robustness of DNNs that are already in use.

DeepFault (Eniser, Gerasimou, and Sen 2019) is another white-box approach for testing DNNs. It uses fault localization, i.e., finding the areas of the network that are mainly responsible for incorrect behaviors. It analyses a trained DNN to find faulty neurons from its hit spectrum analysis using suspiciousness measures. Adversarial inputs are those inputs that achieve high activation values for suspicious neurons. Another popular category of white box methods depends on coverage based techniques. These methods use structural coverage metrics such as neuron coverage and modified condition/decision coverage (MC/DC). These metrics are claimed to be related to faults in neural networks. (Sun et al. 2019) developed a tool which uses MC/DC variants for neural networks and neuron coverage. This tool is used to verify neural networks based on the results of the specified coverage. (Xie et al. 2019) uses mutation based strategies to generate test cases which can maximize neuron coverage. Similarly, (Gao et al. 2020) uses a genetic algorithm based approach which can generate adversarial inputs to maximize neuron coverage and they retrain the DNN simultaneously while generating inputs. (Pei et al. 2017) implements a white-box approach that maximises neuron coverage and differential behaviour of a group of DNNs, implying that different DNNs will produce different output classes for the adversarial input while maximising neuron coverage. (Guo et al. 2018) also focuses on maximising neuron coverage in order to generate adversarial inputs.

Even though the code coverage criteria of software engineering test methodologies corresponds to neuron coverage, it is not a useful indicator of the production of adversarial inputs. Neuron coverage statistics, according to authors in (Harel-Canada et al. 2020), lead to the detection of fewer flaws, making them inappropriate for proving the robustness of DNNs. They also present three new standards – defect

detection, naturalness, and output impartiality – that can be used to gauge the quality of adversarial inputs produced, as alternatives to the L2 and L-inf norms. Their findings establish that the adversarial image set generated by using neuron coverage measures did not perform well on these three standards. Thus, neuron coverage is not a good measure for testing neural networks and generating adversarial images. We have explained these metrics in the following section.

Since our technique relies on finding modifications in DNNs, we also discuss a couple of recent work that is related in this respect. (Goldberger et al. 2020) proposes a technique to find minimal modifications in a single-layer in a DNN, in order to meet a given outcome. This work has been extended further in (Refaeli and Katz 2021) to come up with multi-layer modifications by dividing the problem into multiple sub problems and applying the idea of (Goldberger et al. 2020) on each one of them. Our work proposes an improvement over their idea and uses the improved technique to find small modifications which are then translated into adversarial inputs.

Experimental Setup

We implemented our approach in a tool called AIGENT (Adversarial Input **G**enerator), using the Tensorflow and Keras libraries for working with the DNNs. AIGENT uses Gurobi for constrained optimization.

Benchmark datasets

We conducted our experiments on three popular datasets: MNIST, CIFAR-10, and ImageNet. We chose these benchmarks because they are readily available and are acceptable as inputs by a number of tools, making it easier to compare different techniques in a fair way. MNIST consists of 60,000 black and white images of handwritten digits for the purpose of training and 10,000 for testing. Each image is of 28x28 size. It has 10 classes with labels corresponding to each digit. CIFAR-10 consists of 60000 32x32 colour images in 10 classes. ImageNet is a large dataset which consists of images in 1000 classes.

Metrics of Evaluation

In addition to the usual metrics like L2 and L- ∞ distance, and the time taken, we have used the following metrics to compare our results with the results of existing approaches.

1. Defect detection: to highlight the attack success rate, or the number of benchmarks for which our tool could successfully produce an adversarial image.
2. Naturalness: to score the adversarial images for being admissible, i.e. visibly not very different from the original image. We use Frechet Inception Distance (FID) (Harel-Canada et al. 2020) to measure naturalness. Values of FID close to 0 indicate that the adversarial images are natural, and are therefore desirable.
3. Output impartiality: to reflect whether the adversarial image generation is biased towards any one of the output classes or not. We measure this using the Pielou score (Harel-Canada et al. 2020), which can range from 0 (biased, undesirable) to 1 (unbiased, desirable).

(Harel-Canada et al. 2020) have observed that neuron coverage was negatively correlated with defect detection, naturalness, and output impartiality. Naturalness is considered an essential metric while assessing the quality of adversarial images. Fig. 5 shows how some of the existing methods generate images that perform well on L2 and L- ∞ distance metric, but appear very different from the original image.

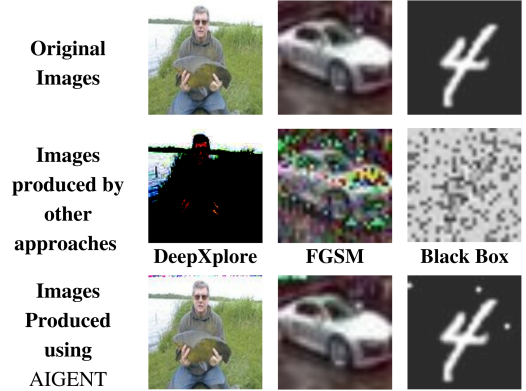


Figure 5: Examples of adversarial images generated by other techniques lacking originality.

Results

Table 1 presents a comparison of AIGENT with other state-of-the-art approaches of generating adversarial images, on all the three benchmark datasets, for several important metrics including FID, Pielou score, defect detection rate, L-2 and L- ∞ distance, and the number of pixels modified. The results demonstrate that AIGENT performs better than all the other approaches in terms of FID, which indicates that the adversarial images generated by our method are natural and visibly quite similar to the corresponding original images. This is further reinforced by the fact that AIGENT modifies far fewer pixels as compared to the other approaches.

Our method could achieve 72% defect detection for MNIST when constraints were stricter. When we allowed the quality of generated adversarial images to degrade slightly in order to achieve a higher defect detection, shown as AIGENT (high defect) in the table, we were able to generate adversarial images for 91.4% of the original images. Our method performs comparable to white box methods. Although black box methods achieve higher defect detection, they modify 100% pixels which leads to visibly distinguishable images. Thus, our method performs well in terms of defect detection, while keeping the modification quite small. Default detection on CIFAR-10 and ImageNet benchmarks for AIGENT was better than all other approaches.

For measuring the Pielou score, we took 50 original images of each class and then calculated the frequency distribution on the classes of adversarial images generated. AIGENT was able to achieve a good Pielou score on all the benchmark datasets. While techniques such as FGSM and DLFuzz have a better Pielou score, it comes at the expense of other metrics such as FID and the percentage of pixels modified. Our

S. No.	Technique	FID	Pielou score	L-2	L- ∞	Time (seconds)	Pixels modified	% of pixels modified	Defect detection
Benchmark dataset: MNIST									
1	AIGENT	0.001	0.725	1.82	0.66	1.726	24	3.06%	72.00%
2	AIGENT (high defect) ¹	0.03	0.74	4.1	0.80	1.799	24	3.06%	91.40%
3	FGSM ²	1.73	0.95	2.8	0.1	0.069	784	100.00%	99.00%
4	Black Box ³	1.98	0.14	6.58	0.23	0.065	784	100.00%	88.40%
5	DeepXplore	0.02	0.47	5.16	1	11.74	60	7.65%	45.66%
6	DLFuzz ⁴	0.17	0.88	2.29	0.39	30	586	74.74%	92.36%
Benchmark dataset: CIFAR-10									
1	AIGENT	0.00009	0.927	1.6	0.5	12.01	12	0.39%	100.0%
2	FGSM ²	0.071	0.92	5.5	0.1	0.079	3072	100.00%	100.0%
3	Black Box ³	0.44	0.703	13.04	0.23	0.082	3072	100.00%	76.20%
Benchmark dataset: ImageNet									
1	AIGENT	0.00011	0.75	6.81	0.73	35	300	0.61%	98.60%
2	FGSM ²	0.43	0.87	22	0.1	0.4	16384	100.00%	97.00%
3	Black Box ³	0.05	0.8	52	0.4	0.3	16384	100.00%	90.00%
4	DeepXplore	0.032	N.A	58.04	0.51	84	15658	95.57%	59.13%
5	DLFuzz ⁴	0.11	N.A	61.1	0.6	57	16102	98.28%	92.00%

Table 1: Comparison of AIGENT with other state-of-the-art techniques on MNIST, CIFAR-10 and ImageNet datasets. Bold values indicate the best figure for each metric. DeepXplore and DLFuzz did not work on CIFAR-10. ¹: Tuned to achieve higher defect detection. ²: Gradient Based technique. ³: (Goodfellow, Shlens, and Szegedy 2015). ⁴: We were getting a few compilation errors in the DLFuzz code (<https://github.com/turned2670/DLFuzz>) which we fixed for this comparison.

method aims at striking a good balance between these metrics as it is crucial for the quality of adversarial images.

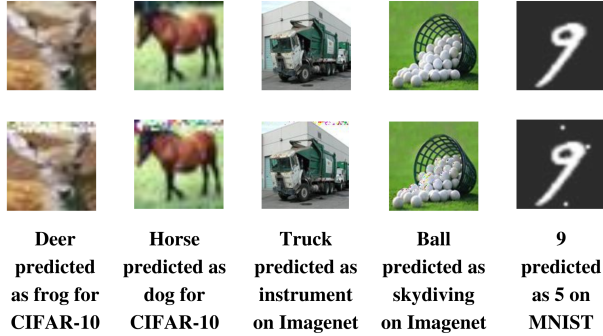


Figure 6: Adversarial images produced by AIGENT (bottom row), and the corresponding original images (top row).

Fig. 6 shows sample adversarial images produced for MNIST, CIFAR-10 and ImageNet datasets. The first row contains original images and the second row contains their corresponding adversarial images. Fig. 7 shows a comparison of AIGENT with black-box, gradient-based, and coverage-guided approaches, on the same input image.

Conclusion

Finding adversarial inputs for DNNs is not just useful for identifying situations when a network may behave unexpectedly, but also for adversarial training, which can make the network robust. We have proposed a technique to generate adversarial inputs via patching of neural networks. In our experiments over three benchmark image datasets, we observed that the proposed method is significantly more ef-

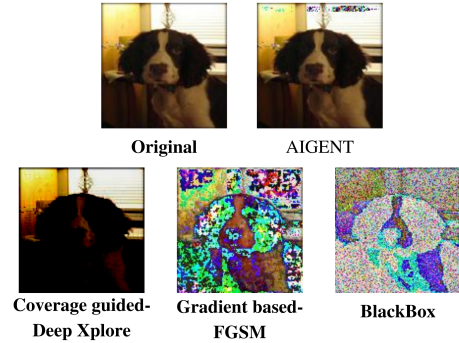


Figure 7: Sample adversarial images from different tools.

factive than the existing state-of-the-art, in terms of the naturalness of the adversarial images as well as the fraction of pixels that were modified.

There are several interesting directions for future work. Since the proposed method works by finding a patch repeatedly, better algorithms for DNN patching would also make our technique more efficient. Another useful direction would be to find a *minimal* patch in order to get the *closest* adversarial example. And even though the technique can, in principle, be applied to DNNs with any activation function, it would be worthwhile to engineer our approach to handle activations other than ReLU efficiently.

References

Alparslan, Y.; Alparslan, K.; Keim-Shenk, J.; Khade, S.; and Greenstadt, R. 2021. Adversarial Attacks on Convolutional Neural Networks in Facial Recognition Domain. Techni-

- cal Report arXiv:2001.11137, arXiv. ArXiv:2001.11137 [cs, eess, stat] type: article.
- Deng, J.; Dong, W.; Socher, R.; Li, L.-J.; Li, K.; and Fei-Fei, L. 2009a. ImageNet: A large-scale hierarchical image database. In *2009 IEEE Conference on Computer Vision and Pattern Recognition*, 248–255.
- Deng, J.; Dong, W.; Socher, R.; Li, L.-J.; Li, K.; and Fei-Fei, L. 2009b. ImageNet: A large-scale hierarchical image database. In *2009 IEEE Conference on Computer Vision and Pattern Recognition*, 248–255.
- Elboher, Y. Y.; Gottschlich, J.; and Katz, G. 2020. An Abstraction-Based Framework for Neural Network Verification. In Lahiri, S. K.; and Wang, C., eds., *Computer Aided Verification - 32nd International Conference, CAV 2020, Los Angeles, CA, USA, July 21-24, 2020, Proceedings, Part I*, volume 12224 of *Lecture Notes in Computer Science*, 43–65. Springer.
- Eniser, H. F.; Gerasimou, S.; and Sen, A. 2019. DeepFault: Fault Localization for Deep Neural Networks. In Hähnle, R.; and van der Aalst, W., eds., *Fundamental Approaches to Software Engineering*, Lecture Notes in Computer Science, 171–191. Cham: Springer International Publishing. ISBN 978-3-030-16722-6.
- Gao, X.; Saha, R. K.; Prasad, M. R.; and Roychoudhury, A. 2020. Fuzz testing based data augmentation to improve robustness of deep neural networks. In *Proceedings of the ACM/IEEE 42nd International Conference on Software Engineering*, 1147–1158. Seoul South Korea: ACM. ISBN 978-1-4503-7121-6.
- Goldberger, B.; Katz, G.; Adi, Y.; and Keshet, J. 2020. Minimal Modifications of Deep Neural Networks using Verification. In Albert, E.; and Kovacs, L., eds., *LPAR23. LPAR-23: 23rd International Conference on Logic for Programming, Artificial Intelligence and Reasoning*, volume 73 of *EPiC Series in Computing*, 260–278. EasyChair.
- Goodfellow, I. J.; Shlens, J.; and Szegedy, C. 2015. Explaining and Harnessing Adversarial Examples. Technical Report arXiv:1412.6572, arXiv. ArXiv:1412.6572 [cs, stat] type: article.
- Gopinath, D.; Wang, K.; Zhang, M.; Pasareanu, C. S.; and Khurshid, S. 2018. Symbolic Execution for Deep Neural Networks. Technical Report arXiv:1807.10439, arXiv. ArXiv:1807.10439 [cs] type: article.
- Guo, J.; Jiang, Y.; Zhao, Y.; Chen, Q.; and Sun, J. 2018. DL-Fuzz: Differential Fuzzing Testing of Deep Learning Systems. In *Proceedings of the 2018 26th ACM Joint Meeting on European Software Engineering Conference and Symposium on the Foundations of Software Engineering*, 739–743. ArXiv:1808.09413 [cs].
- Gurobi Optimization, LLC. 2022. Gurobi Optimizer Reference Manual.
- Harel-Canada, F.; Wang, L.; Gulzar, M. A.; Gu, Q.; and Kim, M. 2020. Is Neuron Coverage a Meaningful Measure for Testing Deep Neural Networks?, 851–862. New York, NY, USA: Association for Computing Machinery. ISBN 9781450370431.
- Krizhevsky, A.; and Hinton, G. 2009. Learning multiple layers of features from tiny images. Technical Report 0, University of Toronto, Toronto, Ontario.
- Kurakin, A.; Goodfellow, I.; and Bengio, S. 2017. Adversarial examples in the physical world. Technical Report arXiv:1607.02533, arXiv. ArXiv:1607.02533 [cs, stat] type: article.
- Li, J.; Liu, J.; Yang, P.; Chen, L.; Huang, X.; and Zhang, L. 2019. Analyzing Deep Neural Networks with Symbolic Propagation: Towards Higher Precision and Faster Verification. In Chang, B.-Y. E., ed., *Static Analysis*, 296–319. Cham: Springer International Publishing. ISBN 978-3-030-32304-2.
- Pang, T.; Xu, K.; Dong, Y.; Du, C.; Chen, N.; and Zhu, J. 2020. Rethinking Softmax Cross-Entropy Loss for Adversarial Robustness. Technical Report arXiv:1905.10626, arXiv. ArXiv:1905.10626 [cs, stat] type: article.
- Pei, K.; Cao, Y.; Yang, J.; and Jana, S. 2017. DeepXplore: Automated Whitebox Testing of Deep Learning Systems. In *Proceedings of the 26th Symposium on Operating Systems Principles*, 1–18. ArXiv:1705.06640 [cs].
- Raj Dhamija, A.; Gunther, M.; and Boulton, T. E. 2019. Improving Deep Network Robustness to Unknown Inputs with Objectosphere. In *Proceedings of the IEEE/CVF Conference on Computer Vision and Pattern Recognition (CVPR) Workshops*.
- Refaeli, I.; and Katz, G. 2021. Minimal Multi-Layer Modifications of Deep Neural Networks. *ArXiv*, abs/2110.09929.
- Sun, Y.; Huang, X.; Kroening, D.; Sharp, J.; Hill, M.; and Ashmore, R. 2019. DeepConcolic: Testing and Debugging Deep Neural Networks. In *2019 IEEE/ACM 41st International Conference on Software Engineering: Companion Proceedings (ICSE-Companion)*, 111–114. ISSN: 2574-1934.
- Wang, S.; Pei, K.; Whitehouse, J.; Yang, J.; and Jana, S. 2018. Formal Security Analysis of Neural Networks Using Symbolic Intervals. In *Proceedings of the 27th USENIX Conference on Security Symposium, SEC'18*, 1599–1614. USA: USENIX Association. ISBN 9781931971461.
- Xie, X.; Ma, L.; Juefei-Xu, F.; Xue, M.; Chen, H.; Liu, Y.; Zhao, J.; Li, B.; Yin, J.; and See, S. 2019. DeepHunter: a coverage-guided fuzz testing framework for deep neural networks. In *Proceedings of the 28th ACM SIGSOFT International Symposium on Software Testing and Analysis*, 146–157. New York, NY, USA: Association for Computing Machinery. ISBN 978-1-4503-6224-5.
- Yang, P.; Li, J.; Liu, J.; Huang, C.-C.; Li, R.; Chen, L.; Huang, X.; and Zhang, L. 2021. Enhancing Robustness Verification for Deep Neural Networks via Symbolic Propagation. *Formal Aspects of Computing*, 33(3): 407–435.